AN INVESTIGATION INTO THE EFFECT OF THE MANUFACTURING PROCESS ON THE FATIGUE PERFORMANCE OF CONVEYOR PULLEYS

G Styger and R F Laubscher

University of Johannesburg

1. INTRODUCTION

Pulleys are critical items in belt conveyors. Their primary role is to drive large mining conveyor systems, facilitating the transportation of ore over extensive distances, both in South Africa and abroad. The effect of the manufacturing process (with specific emphasis on the induced residual stresses) on the fatigue performance of conveyor pulleys is herein investigated and reported. Early researchers investigated the design of the pulleys and the relevant components making up the assembly. Their work concentrated on the analysis of the individual components and not the effect on each other as an integral unit, based on the numerical methods available at the time. Finite element analysis (FEA) allows for the investigation of the pulley as a complete structurally-integrated unit. This facilitates the determination of the in situ deformation and stresses in the pulley, due to the induced assembly and operational loads. The manufacturing process of the pulleys requires extensive metal forming and joining methods. The finished product is then stress relieved typically if the shaft size is above a pre-determined size.

An investigation was undertaken to study these effects by virtue of a testing program to determine the residual stress state in the relevant components. The processes of interest include the roll bending of the cylindrical shell, the machining of the end disks and the welding of the end disks to the shell. The effect on the reduction of the residual stresses, with regards to stress relieving, is also investigated for the assembly. The testing program consisted of the fabrication of two roll bent cylindrical plates of a pre-selected size, using the same joining techniques (sub-arc welding) as used for the pulleys. The sample was then split into separate samples. One sample was sent for stress relieving.

The incremental hole drilling technique was used to determine the residual stresses at the surface of the welded plates. Equally spaced measuring positions were considered in the transverse direction (across the plate and the weld bead), thus evaluating the residual stress in the surface of the plate, due to roll bending and welding respectively. The residual stress measurement was conducted for both the stress relieved and as-built condition. The material properties of the mild steel used for construction were determined by tensile tests of the 350 WA plate specimens. An FE model of a pre-selected T-Bottom type pulley would then be developed, including the assembly and operational loads. The measured residual stresses would then be added to the calculated stress via superposition. The effect on the fatigue resistance of the critical areas of the pulley are estimated with the residual stresses included and excluded and comparisons made. Conclusions and recommendations are drawn and presented.

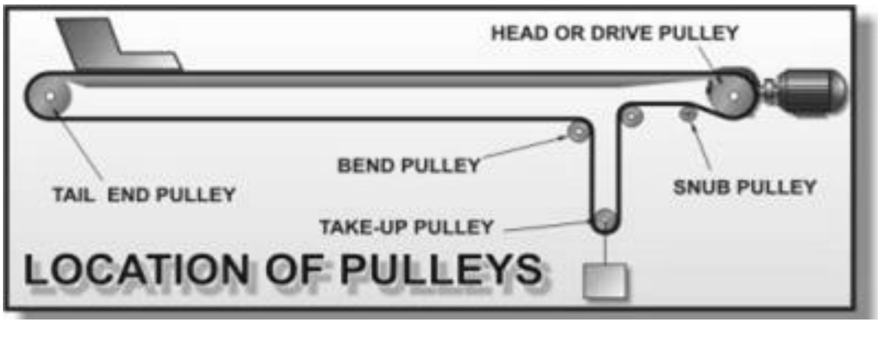

Figure 1. Locations of pulleys in the conveyor system [1]

2. DEVELOPMENT OF THE DESIGN OF CONVEYOR PULLEYS

The design of conveyor pulleys dates back to the 1930's and 1940's when the classical theory of plates and shells was utilised. The research that was to follow in the 1960's and 1970's in Germany would set the benchmark for the fundamental development of the understanding of the behaviour of the pulley, still used today.

Lange [2] was the first to formalise the representation of the triaxial stress state in the pulley shells and end disks as a Fourier series expansion. Schmoltzi [3] investigated the contact stress field of the keyless locking element connections used between the shaft and pulley, which became popular at the time. These investigators also conducted extensive strain gauging to verify their work.

King [4] developed a design procedure for the pulleys that could be utilised in a drawing office. His work considered both steady-state static and fatigue conditions of the pulley. His work is still extensively used by industry. Qiu et al. [5] developed a new pulley stress analysis system based on the modified matrix method. The system allowed for simpler analysis than was possible with Finite Element Analysis (FEA) at the time. It was also able to correctly determine the complex stress state at the shell-to-end disk interface not previously possible. The integrated analysis of the pulley and shaft as in FEA was possible. Sethi et al. [6] described the Conveyor Dynamics, Inc. (CDI) design criteria of pulleys with a test case investigated empirically as well as with FEA and experimental work. Experience based on failure analyses was also discussed.

The current empirical methods do not consider the pulley as an integral unit with all the components having an influence on each other. The modified matrix method and FEA are the only methods that allow the pulley manufacturer to accurately assess the appropriateness of the design of the pulley. Further to this, the effect of stress relieving the pulley is not included in the design criteria currently used. This paper aims to assess this effect on the performance of a pulley.

3. MANUFACTURING PROCESS OF CONVEYOR PULLEYS

The manufacturing process of the conveyor pulley consists of the assembly of a number of machined and fabricated components.

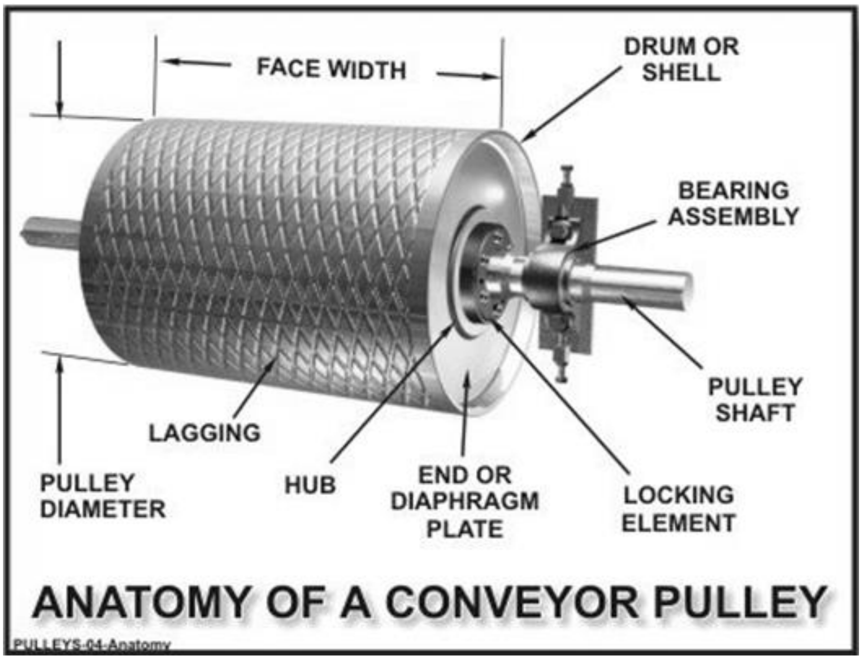

Figure 2. Components of the conveyor pulley [7]

The components are produced from the following manufacturing procedures:

- A length of bright bar of mild steel is cut to length and then machined into a shaft
- The locking element is typically machined in-house or it is a bought-out item
- The end plate/disk is cut and machined from SANS 1431 350 WA plate. A turbine or T-Bottom type end disk is machined depending on the loading and size of the pulley required for the application.

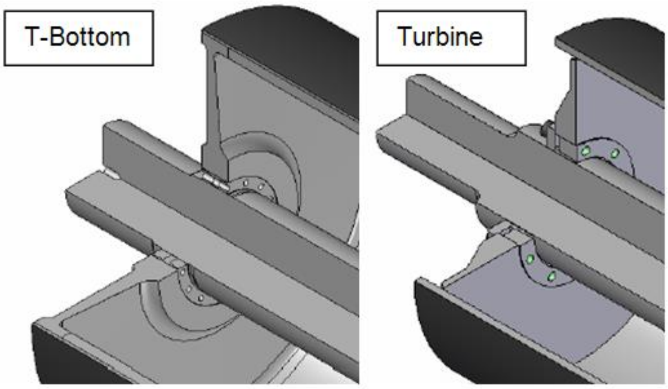

Figure 3. T-bottom and turbine type end disks

- The shell is cut from 350 WA plate and then roll bent to form a pipe. A double butt seam weld is used to join the ends of the shell
- The turbine type end disk is inserted into the shell from each end a specified distance and then a submerged arc single butt weld is used to join it to the shell
- The T-Bottom type end disk is joined to the ends of the shell with a submerged arc double butt weld.

The locking elements are then placed onto the shaft, which is in turn placed into the pulley shell. The bolts of the locking elements are then tightened to the specified torque thus inducing the appropriate interface pressure to prevent slip and disassembly during operation.

4. EXPERIMENTAL WORK

An experimental program was set up to assess the residual stress state in the critical welds of the shell. The residual stresses set up due to the machining operations of the end disks and shaft is not considered in the study.

The program consisted of the roll bending of two cylinders of a predetermined size. Sub-merged arc welding of the longitudinal and circumferential seams was conducted as per the specification for manufacturing a T-Bottom type shell along with the roll bending of the shell. The flange of the end disk and shell of the pulley was considered, each being of equal length.

Figure 4. Completed fabrication of the shell

4.1 Mechanical Properties

Tensile tests were conducted to determine the mechanical properties of the SANS 1431 GR 350 WA plate as used for the shells and end disks. The tests were performed according to ISO 6892:1998.

Modulus of Elasticity (GPa)	200.00
Poisson's Ratio	0.3
Proportional Limit (MPa)	299.23
0.2% Off-Set Yield Strength (MPa)	390.77
Upper Yield Strength (MPa)	395.39
Lower Yield Strength (MPa)	390.44
Ultimate Tensile Strength (MPa)	479.53

Table 1. Mechanical properties of 350 WA

4.2 Stress Relieving of the Shell

The shell was split in two, and the one half was sent for stress relieving. This was done in order to measure the as-welded and stress relieved residual stresses in each section respectively.

Holding Temperature (°C)	Time (hrs)
600	4

Table 2. Holding temperature for the stress relieving

4.3 Residual Stress Measurement

The residual stress measurements of the welds were conducted with the use of the incremental hole drilling method. Residual stresses are inherent in many components due to the manufacturing process. They are said to be 'self-equilibrating' stresses as they are in equilibrium within the component without external loads [8].

For equilibrium to exist, both tensile and compressive residual stresses must be present in order to satisfy equations of internal force and moment equilibrium. This complies as follows:

$$\sum F = \sum M = 0$$

They are caused by different production methods. A mechanical method such as bending of sheet metal upon removal of the load spring back occurs and residual stresses remain in the part. Thermal methods such as welding induce non-uniform temperature gradients which cause thermal expansion and contraction contributing to elastic/plastic deformations producing triaxial residual stresses. This reduces the fatigue resistance of the welded assembly. Machining operations such as turning, milling and grinding affect fatigue resistance of the part. Cold working and possible phase transformations contribute to the development of residual stress in these processes [8].

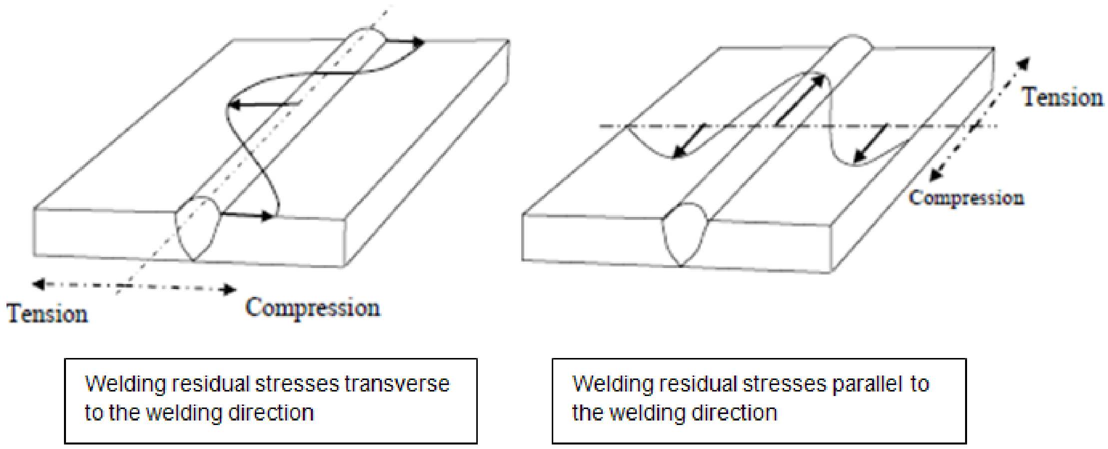

Figure 5. Longitudinal and transverse residual stresses in a single butt weld [9]

The incremental hole drilling method is one of the most widely used techniques for measuring residual stress. It is relatively simple, affordable and versatile. The equipment can be used in the laboratory and out in the field. The hole drilling principle was first proposed by Mathar [10] in 1934 and since then many investigators have developed the method resulting in the standard procedure ASTM E837 [11] being formalised to assist researchers.

The technique involves the introduction of a small hole into a component containing residual stresses or under preload. The subsequent local relieved surface strains are measured with the use of a specifically designed strain gauge rosette. The residual stresses are then calculated from the relieved strains in conjunction with specific calibration constants derived from experimental and Finite Element Analyses.

In practise, the method involves the increment drilling of a hole in the centre of the strain gauge rosette, recording the relieved strains at each depth increment. The incremental measurement of the relieved strains allows stress gradients to be measured through the depth. This may be essential when trying to ascertain the residual stresses generated due to shot peening which has an abrupt stress gradient directly under the surface. Uncertainties such as surface roughness, hole diameter and eccentricity as well as user skill affect the accuracy of the method.

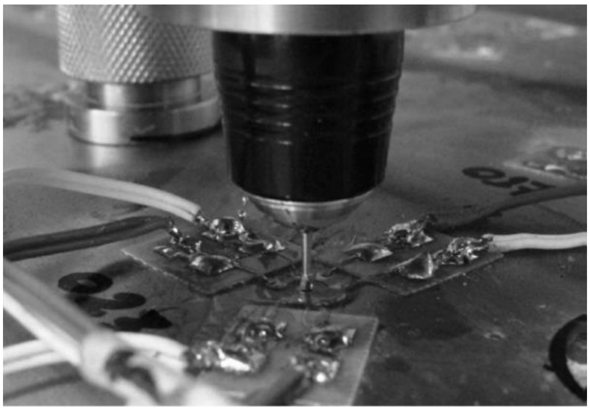

Figure 6. Drilling through the centre of the strain gauge rosette [12]

4.4 Experimental Set-up for the Residual Stress Measurement

The experimental set-up of the residual stress measurement of the welds involved particular steps for the required output. A quantitative study was conducted to determine the level of residual stresses in both the as-welded and stress relieved states for strategic positions of the split shell samples.

The measurement positions were selected at the weld toes of the circumferential butt welds in order to determine the residual stress due to welding in the longitudinal and transverse directions. The residual stress in the transverse direction is of particular interest as this would be used for the fatigue assessment at the weld toe. Residual stress was additionally measured a distance away from the weld as this would allow the measurement of the residual stress due to the roll bending in the shell.

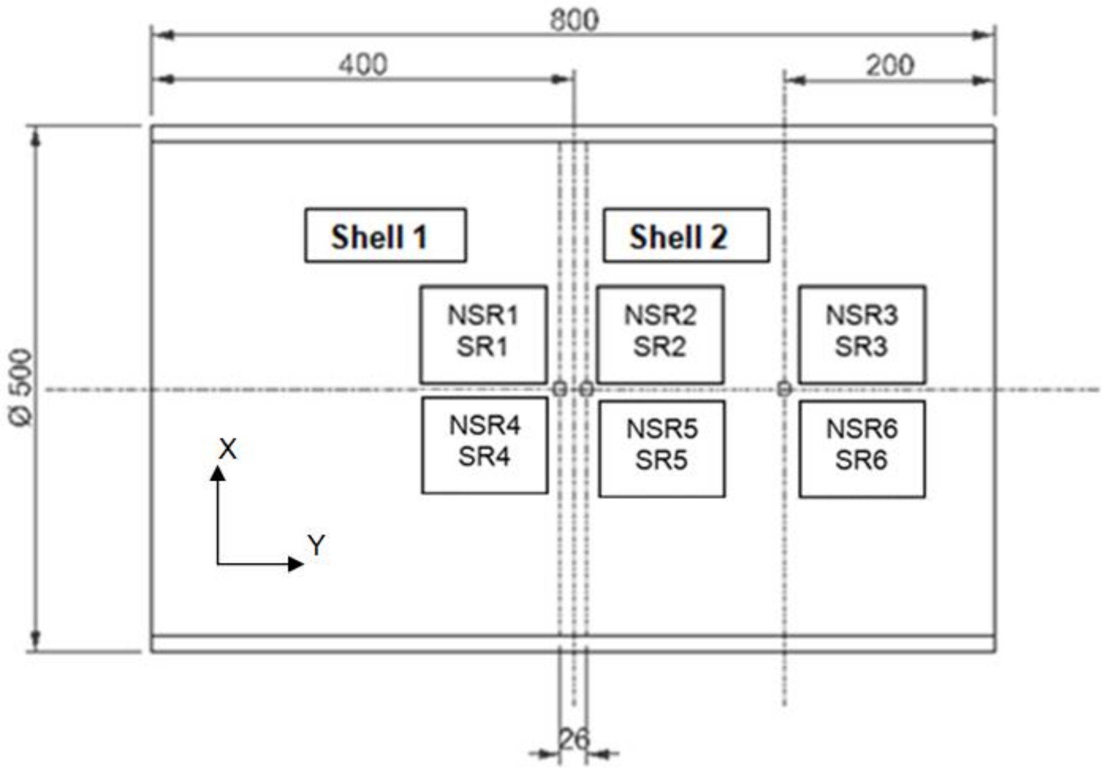

Figure 7. Measurement positions on the inside and outside diameter

The labelling convention refers to the as-welded and stress relieved conditions. The 'NSR' pertains to the non-stress relieved or as-welded state. The 'SR' pertains to the stress relieved state. The measurement positions 1, 2, 4 and 5 are on the weld toes of either side of the circumferential weld. The measurement positions 3 and 6 are on the parent material of the shell to determine the residual stress due to the roll bending of the plate.

The split shell samples were manufactured according to the recommended procedure for T-Bottom type pulleys.

4.5 Results of the Residual Stress Measurement

Uniform and non-uniform residual stress calculations were performed as per ASTM E837-08 [11] of the relevant measurement positions. Both calculations were conducted in order to ascertain whether the stress distribution through the hole depth at the weld toes were uniform or not. Previous studies have shown that residual stresses as produced by welding are typically non-uniform with respect to depth [13]. Hence the non-uniform stress method [11] is most appropriate for this application and was used in this study.

The non-uniform stress calculations for the as-welded and stress relieved condition of the butt welds revealed the following results:

	As-welded			**Stress-relieved**		
	Weld Pos.	Stress-XX (MPa)	Stress-YY (MPa)	Weld Pos.	Stress-XX (MPa)	Stress-YY (MPa)
Description	**Roll-Bent Plate**					
Inner Dia.	NSR3	142.7	75.0	SR3	50.3	37.6
Outer Dia.	NSR6	-175.8	-117.8	SR6	11.1	7.4
	Weld Toe					
Inner Dia.	NSR1	330.2	166.6	SR1	62.5	61.4
Inner Dia.	NSR2	361.0	332.5	SR2	47.1	45.8
Outer Dia.	NSR4	174.9	73.5	SR4	-49.8	-6.7
Outer Dia.	NSR5	244.2	-35.2	SR5	61.2	40.2

Table 3. ASTM E837-08 Non-uniform stress results for the as-welded and stress relieved conditions

The maximum residual stress for the as-welded condition was 361 MPa based on the non-uniform stress method, for the NSR2 measurement position. This was for the residual stress parallel to the weld. The maximum residual stress for the stress relieved condition was 62.5 MPa based on the non-uniform stress method, for the SR1 measurement position. The results indicate a large reduction in residual stress after stress relieving, however the residual stresses are still tensile in areas and hence could have a negative impact from a fatigue point of view.

It must be noted that the residual stress measurements for the fatigue assessment are assumed to be the same around the circumference of the joints both in the hoop and axial directions for this study.

5. NUMERICAL WORK

A numerical program was set up for the Finite Element Analysis of a preselected T-Bottom type pulley to determine the steady-state static stresses under the operational and assembly loads induced. The pulley was selected based on the following assumptions and conditions.

- A pulley/shell with an outside diameter of 500 mm and 16 mm thick was selected to facilitate lower transportation costs. In addition, the smaller size allowed for easy of movement within the laboratory.
- A belt speed of 2.5 m/s was used in the determination of the number of rotation cycles for the fatigue assessment.
- A belt tension of 130 kN and an angle of wrap of 15 degrees was selected in order to induce local deflections and stresses in the shell of the pulley.

- The pulley is assumed to behave as if placed in the snub position and hence is a non-drive pulley. Therefore, self-weight, resultant tension and the induced pressure of the locking elements are the only load cases.
- The tensioning up of the locking elements is not considered directly in the analyses. The induced pressure for the shaft and the end disk is selected from the catalogue [14] and applied and run as a separate analysis.
- A complete integral analysis of the pulley is conducted with the pulley shell, locking element and shaft being modelled. The locking elements and shaft are modelled in order to contribute correctly to the stiffness of the structure as well as the accurate determination of the bending moments for the end disks and shell of the pulley.
- Operational loads are considered in the analyses and start-up conditions are not considered due to the low number of start-ups experienced during the pulley's life [15]. The von Mises stress should not exceed the yield strength of the material with a suitable factor of safety under start-up conditions.

5.1 Methods Used for the Stress Analysis of a Pulley

Currently pulleys are designed with the methods determined by Lange [2], Schmoltzi [3] and King [4] by the manufacturers. Finite element analysis of the pulleys is often only performed when T-Bottom type pulleys are used due to the complex shape of the end disk or if the project house/mine has requested a study. The modified matrix method developed by Qui et al. [5] and compared with FEA are techniques that correctly deal with the relative stiffness's at the end disk-to-shell interface thus determining the stress ranges in this critical area, which is often welded and thus a site of potential fatigue crack initiation. The former methods consider the pulley and shaft separately. This can result in conservative determinations of shaft diameters and shell thicknesses.

Early finite element analysis work of Sethi et al. [6] and other workers focused on the Fourier analysis of pulleys as a full 3D analysis of a pulley was not possible due to computational limitations. The Fourier analysis uses a meshed 2D axisymmetric structure and allows non-axisymmetric loading such as belt pressure due to belt tension of a pulley to be analysed.

Both 3D and Fourier analyses of the pulley were conducted and compared in this study.

5.2 The Finite Element Analysis System

The LUSAS$^{@}$ Finite Element Analysis system was used for the 3D and Fourier analyses of this preselected pulley [16].

The 3D analysis of the pulley was conducted with the use of hexahedral brick elements with linear element interpolation. Due to computer limitations, elements with quadratic element interpolation were not run. The result of the 3D analysis was used as the benchmark for the assessment of the accuracy of the Fourier analysis conducted.

As stated above, the Fourier analysis is used to represent an axisymmetric structure subjected to non-axisymmetric loading. The method is semi-analytical. The loading is defined circumferentially with a Fourier series. The displacements defining the circumferential behaviour are in turn defined with a Fourier series. The axisymmetric in-plane deformations are defined by the finite element formulation [17].

The circumferential variations of the loads and structural displacements are defined as the sum of the harmonics of a Fourier series. The number of harmonic components determines the number of times the analysis is run. The solutions are then combined based on the principle of superposition for the overall solution. The results can then be plotted for each circumferential position of the user's choice.

The use of this semi-analytical approach allows the three dimensional analysis to be reduced to a series of two dimensional analyses, with the saving in solving effort being dependent upon the number of harmonics required to accurately reproduce the structural response of the 3D structure.

Mesh sensitivity analyses should always be conducted to determine the size of the elements required to achieve convergence of the solution. This was conducted for the 3D, axisymmetric and Fourier analyses.

5.3 Number of Fourier Harmonic Components to Consider

An investigation into the number of Fourier harmonic components required for the accurate analysis of the pulley was conducted. This was required as an increased number of Fourier harmonic components would lead to a better representation of the loading of the structure but with increased computational cost. The computational cost is directly proportional to the number of Fourier harmonic components considered.

Sethi et al. [6] found that for an angle of wrap close to 180 degrees, the increase in accuracy of going from 15 to 35 harmonic components was marginal, typically less than 1%. However, they found that when the angle of wrap was less than 20 degrees, more than 35 harmonic components were required to sustain the same level of accuracy.

The results of the analyses to determine the appropriate number of harmonic components is as follows:

The percentage difference was determined to ascertain the level of convergence. The target value is the maximum vertical displacement of 0.17487 mm as determined from the 3D analysis of the pulley.

$$PD = \frac{MRD - TV}{TV}$$

Number of the Harmonics	Mesh Size (mm)	Element Interpolation	Maximum Radial Displacement (mm)	Percentage Difference	Time (min)
18	4	Quadratic	-0.174767	-0.059%	0.967
36	4	Quadratic	-0.174779	-0.052%	2.083
54	4	Quadratic	-0.174776	-0.054%	2.950
72	4	Quadratic	-0.174777	-0.053%	3.950

Table 4. The results of the harmonic component assessment

The assessment revealed small changes between the results as the number of harmonics were increased for the chosen mesh size of 4 mm with quadratic interpolation. The results indicate a total of 54 harmonic components should be selected based on accuracy and run time.

5.4 Geometry of the Pulley

The geometry of the preselected pulley was defined based on the assumptions and conditions previously stated. The following components were modelled:

- The pulley shell consisting of the shell, end disks and double butt welds as an integral unit.
- The shaft was modelled in order to accurately model the stiffness's of the pulley but was not considered in the fatigue assessment of the pulley.
- The locking elements were considered as a solid connection between the shaft and end disk.

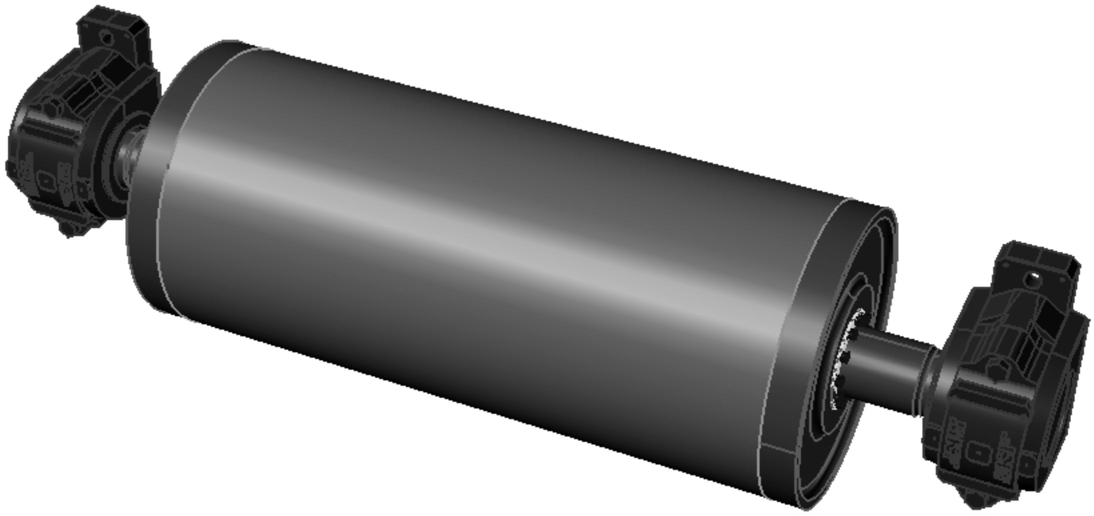

Figure 8. Overall geometry of pulley

Diameter of the Pulley	500 mm[1]
Pulley Face Width	1 200 mm
Bearing Centre Distance	1 700 mm
Length of Shaft	1 826 mm

Table 5. Overall dimensions of the pulley

Note 1: The overall diameter excludes the additional thickness due to the lagging. The lagging is not included in the analysis.

The overall dimension of the simplified geometry of the pulley used for the analyses is indicated in Figure. A quarter of the model is used to indicate the dimensions more clearly:

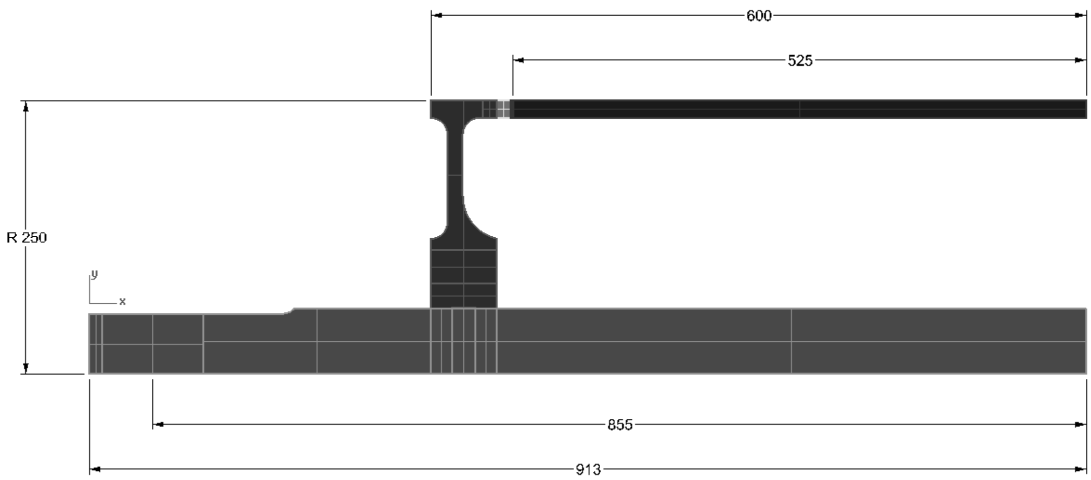

Figure 9. Simplified geometry of the pulley used for the analyses

5.5 Loading and Boundary Conditions of the Pulley

The loading of the pulley model consists of self-weight, belt pressure and locking element interface pressure. Built-in and simply supported conditions were used for the models assessed.

The belt pressure is determined from the belt tension and dimensions of the pulley. King [4] proposed the following equation for the determination of belt pressure suitable for a non-drive pulley . It is as follows:

$$Pb = \frac{2T}{WD}$$

The belt pressure is therefore 0.495 MPa.
The belt pressure is applied as a step function over the circumference of the pulley for the specified belt width which is shown in Figure 10:

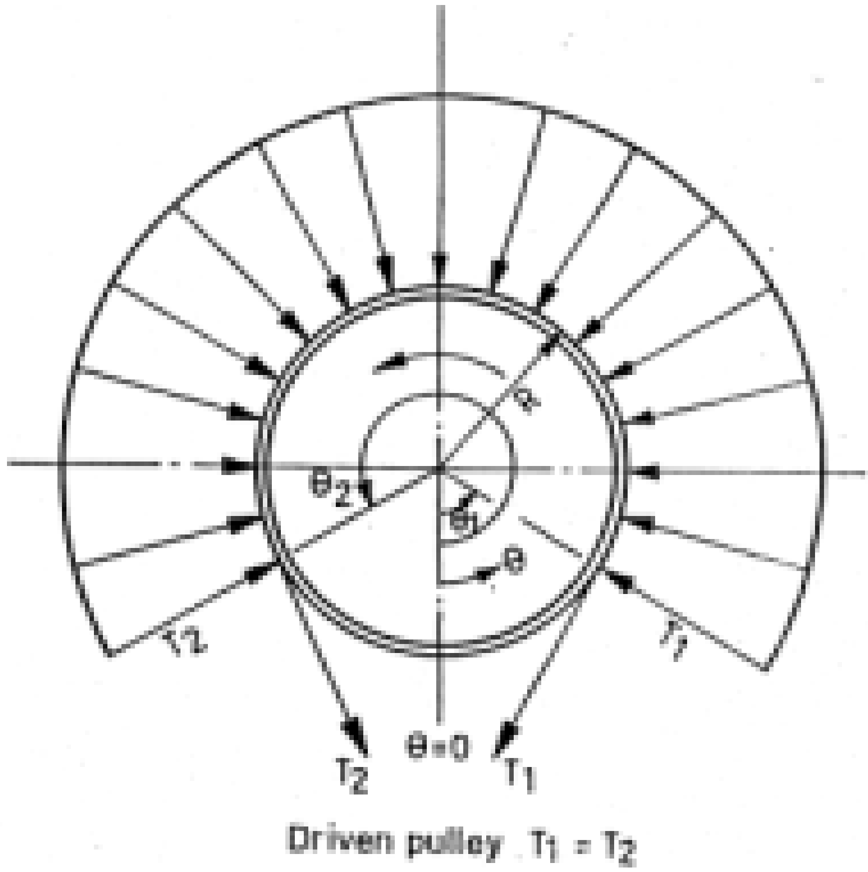

Figure 110. Belt pressure distribution over the circumference of a driven pulley [18]

The circumferential belt pressure distribution used for the mesh sensitivity analysis is shown as follows:

Circumferential Position (Degrees)	Radial Pressure (MPa)
0	0.495
15	0.495
15.001	0.000
360	0.000

Table 6. Circumferential belt pressure for the mesh sensitivity analysis

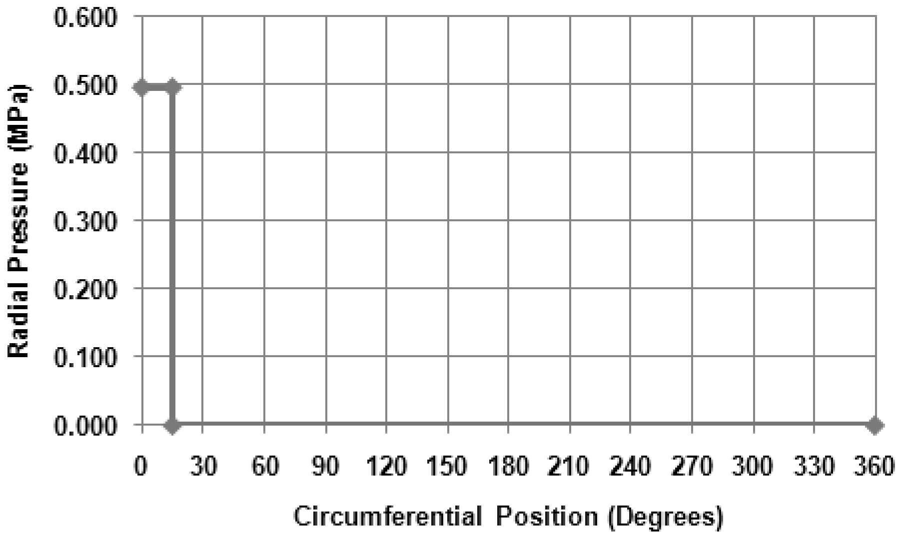

Figure 11. Graph of the belt pressure vs circumferential position for the mesh sensitivity analysis

The circumferential belt pressure distribution used for the final Fourier analysis is shown as follows:

Circumferential Position (Degrees)	Radial Pressure (MPa)
0	0.000
172.499	0.000
172.499	0.495
187.5	0.495
187.501	0.000
360	0.000

Table 7. Circumferential belt pressure for the final Fourier analysis

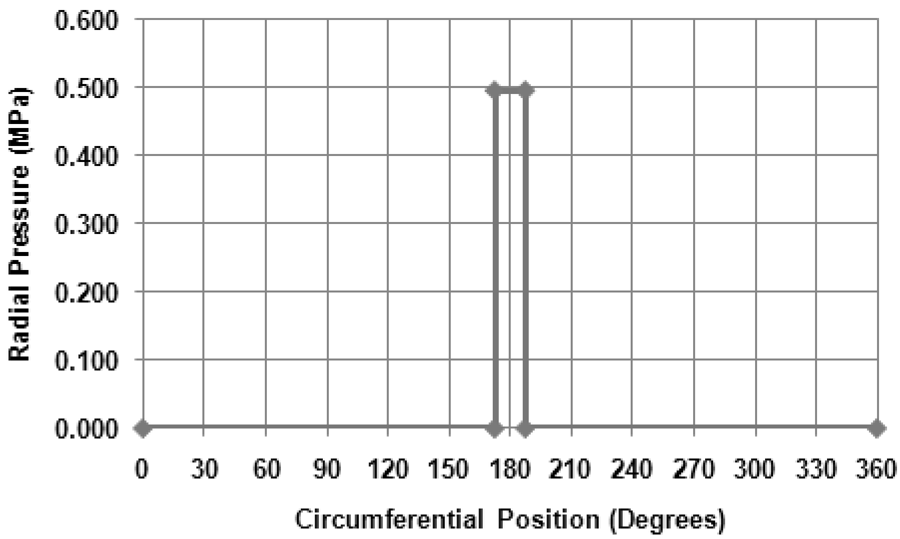

Figure 12. Graph of the **b**elt pressure vs circumferential position for the final Fourier analysis

The belt tension across the width may be applied as linear distribution or as a sinusoidal function as proposed by Lange [2]. The various functions of the belt tensions applied over the width are shown in Figure 14:

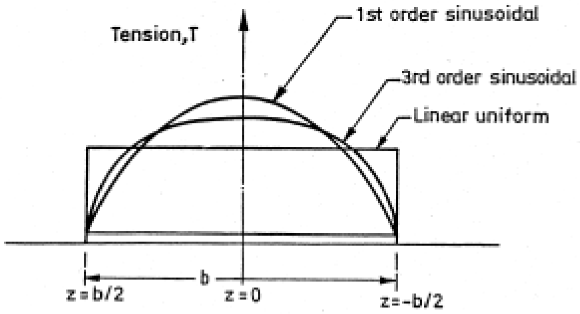

Figure 13. Various functions used to apply the belt pressure over the belt width [18]

The linear uniform belt pressure was assumed over the belt width for the 3D and Fourier analyses.

The belt pressure was applied to the model as shown in Figure 14:

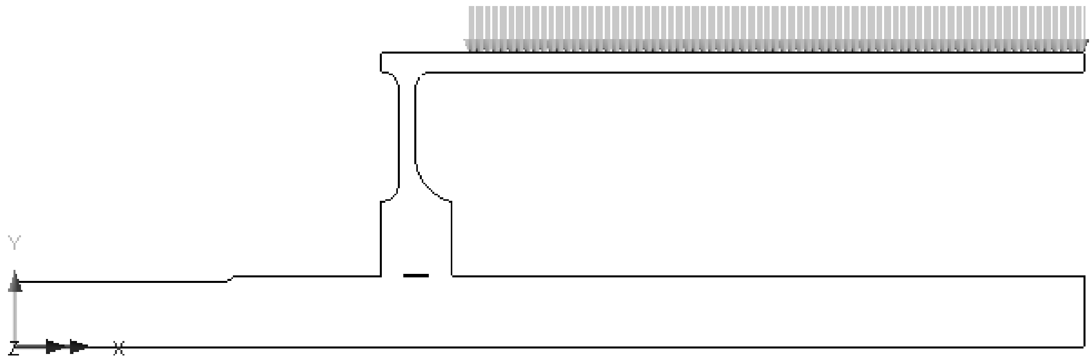

Figure 14. Belt pressure applied to the model

The locking element pressure interface pressure for the end disk of 122 MPa and 188 MPa for the shaft was applied as shown in Figure 15.

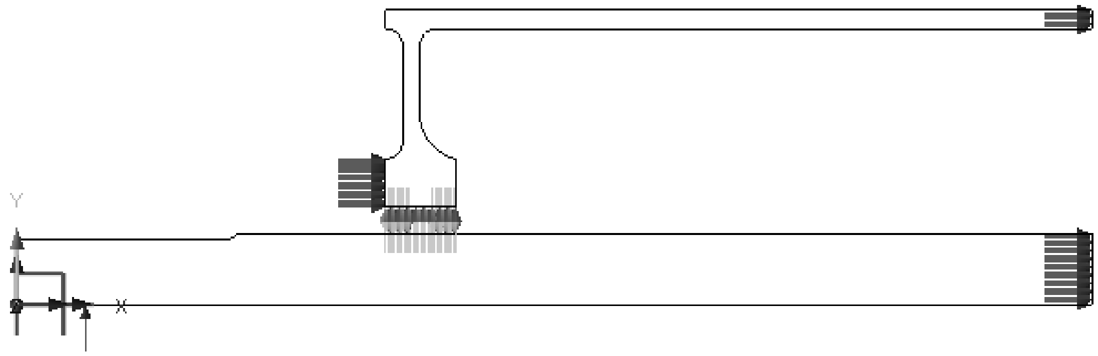

Figure 15. Locking element interface pressure applied to the model for the end disk and shaft

This load case was run as an axisymmetric analysis. These results were then added by superposition to the Fourier analysis that was conducted. The axisymmetric analysis determined the mean stress in the pulley due to the assembly load case.

The built-in boundary condition of the pulley was used for the mesh sensitivity and harmonic component assessment as shown in Figure 16:

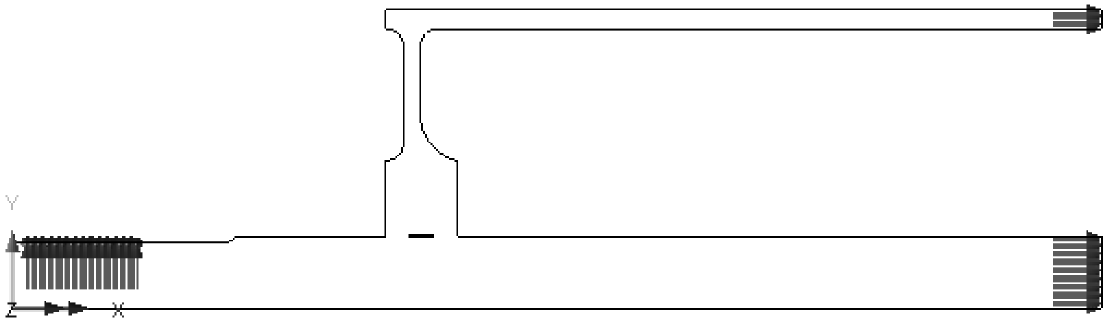

Figure 16. Built-in boundary conditions for the mesh sensitivity and harmonic component assessment

The simply supported boundary condition was used for the final analysis of the pulley once the mesh sensitivity and harmonic component assessment had been completed as shown in Figure 17:

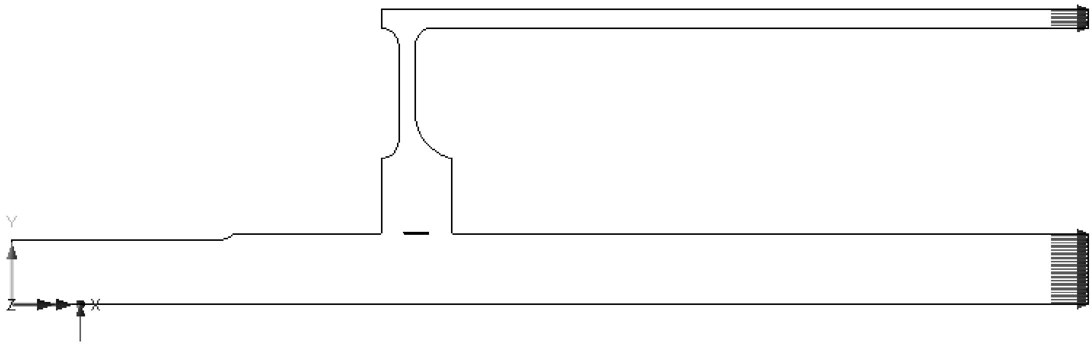

Figure 17. Simply supported boundary condition of the final analysis of the pulley

5.6 3D Analysis of the Pulley

The 3D analysis of the pulley involved a mesh sensitivity assessment to determine the appropriate element size required to achieve convergence. The maximum vertical displacement was reported from the solution. A quarter of the model was run with self-weight and belt pressure being considered in the analysis. The assembly load due to the locking element pressure load case was not considered for this analysis.

The geometry, boundary and loading conditions of the 3D quarter model are shown in Figure 18:

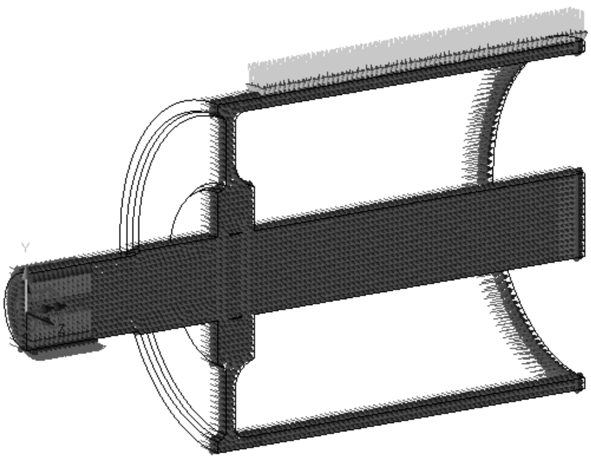

Figure 18. Quarter model for the 3D analysis

The result of the mesh sensitivity analysis is shown in Table 8:

Mesh Size (mm)	Element Interpolation	Maximum Radial Displacement (mm)	Time (min)
16	Linear	-0.17264	0.383
8	Linear	-0.17503	15.250
8	Linear	-0.17487	41.200

Table 8. 3D mesh sensitivity results

The 3D model was run with a sub-divided mesh with an element size of 8 mm. Linear element interpolation was used. This solution revealed a maximum vertical displacement of 0.17487 mm in a run time of 41.2 minutes. Reduced mesh sizes for linear and quadratic element interpolations of the hexahedral mesh were not possible due to computer hardware limitations. The final result obtained is adequate for the study performed.

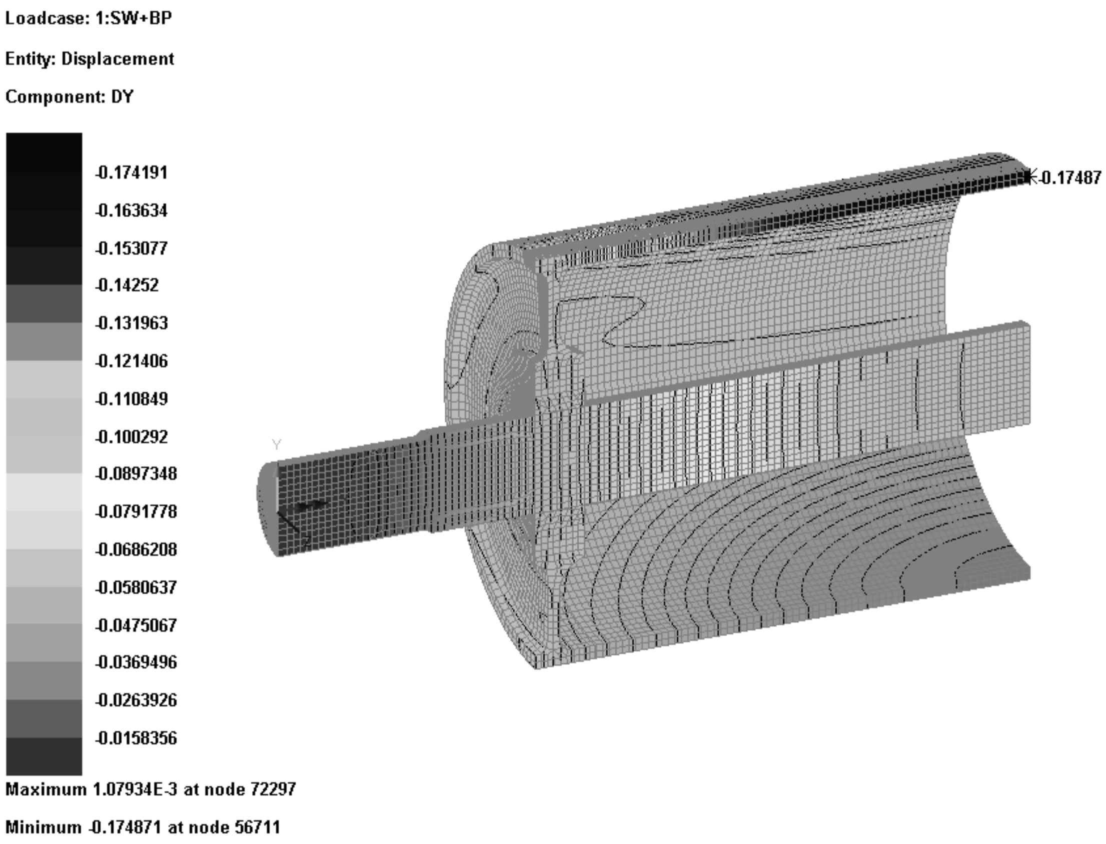

Figure 19. Contour plot of the maximum vertical displacement for the 3D analysis

5.7 Axisymmetric Analysis of the Pulley

The axisymmetric analysis of the pulley was conducted in order to ascertain the effect of the assembly stresses due to the interface pressure of the locking elements. These results would then be used with the operational and residual stress results to determine the influence on the fatigue performance of the pulley.

A mesh sensitivity assessment was conducted in order to determine the appropriate mesh size and element interpolation to be used to achieve convergence. The level of convergence was determined based on the percentage difference with the target value being the interface hub pressure of 122 MPa for the locking element.

$$PD = \frac{IHP - TV}{TV}$$

Mesh Size (mm)	Element Interpolation	Radial Stress (MPa)	Percentage Difference	Time (min)
16	Linear	74.6	-38.84%	0.0167
8	Linear	94.9	-22.24%	0.0167
4	Linear	107.5	-11.90%	0.0333
2	Linear	114.5	-6.13%	0.300
16	Quadratic	119.1	-2.34%	0.0167
8	Quadratic	121.2	-0.66%	0.0167
4	Quadratic	121.8	-0.18%	0.0667
2	Quadratic	121.9	-0.05%	0.850

Table 9. Mesh sensitivity results for the axisymmetric analysis

The mesh sensitivity study revealed that the analyses with quadratic element interpolations yielded the most accurate results. A mesh size of 4 mm with quadratic element interpolation was used for the final analysis due to the optimal balance of accuracy with run time.

5.8 Fourier Analysis of the Pulley

The Fourier analysis of the pulley was conducted in order to ascertain the effect of the self-weight and the belt pressure on the pulley. These results would then be used with the assembly and residual stress results to determine the influence on the fatigue performance of the pulley.

A mesh sensitivity assessment was conducted in order to determine the appropriate mesh size and element interpolation to be used to achieve convergence. The level of convergence was determined based on the percentage difference with the target value being the maximum radial displacement of the pulley.

$$PD = \frac{MRD - TV}{TV}$$

*****The target value is the maximum vertical displacement of 0.17487 mm from the converged 3D analysis of the pulley.

Mesh Size (mm)	Element Interpolation	Number of Harmonics	Maximum Radial Displacement (mm)	Percentage Difference	Time (min)
16	Linear	54	-0.15278	-12.63%	0.050
8	Linear	54	-0.16802	-3.92%	0.133
4	Linear	54	-0.17281	-1.18%	0.883
2	Linear	54	-0.17433	-0.31%	5.217
16	Quadratic	54	-0.17333	-0.88%	0.083
8	Quadratic	54	-0.17452	-0.20%	0.417
4	Quadratic	54	-0.17473	-0.05%	1.917
2	Quadratic	54	-0.17490	0.02%	16.967

Table 10. Results of the mesh sensitivity assessment of the Fourier analysis

The mesh sensitivity study revealed that the analyses with quadratic element interpolations yielded the most accurate results. A mesh size of 4 mm with quadratic element interpolation was used for the final analysis due to the optimal balance of accuracy with run time.

5.9 Final Fourier Analysis of the Pulley

The final Fourier analysis was run with the simply supported boundary conditions with the self-weight and belt pressure load cases. The mesh size, element interpolation and number of harmonic components as previously determined were used in this analysis.

The results of this final analysis for the pulley shell for the circumferential position of 180 degrees is shown in Table 11:

Result Quantity	Value of the Result
Maximum Radial Displacement (mm)	-0.351
von Mises Stress (MPa)	35.5
Stress-XX (MPa)	21.0

Table 11. Results of the final analysis

The contour plot of the maximum radial displacement of the pulley shell is shown in Figure 20:

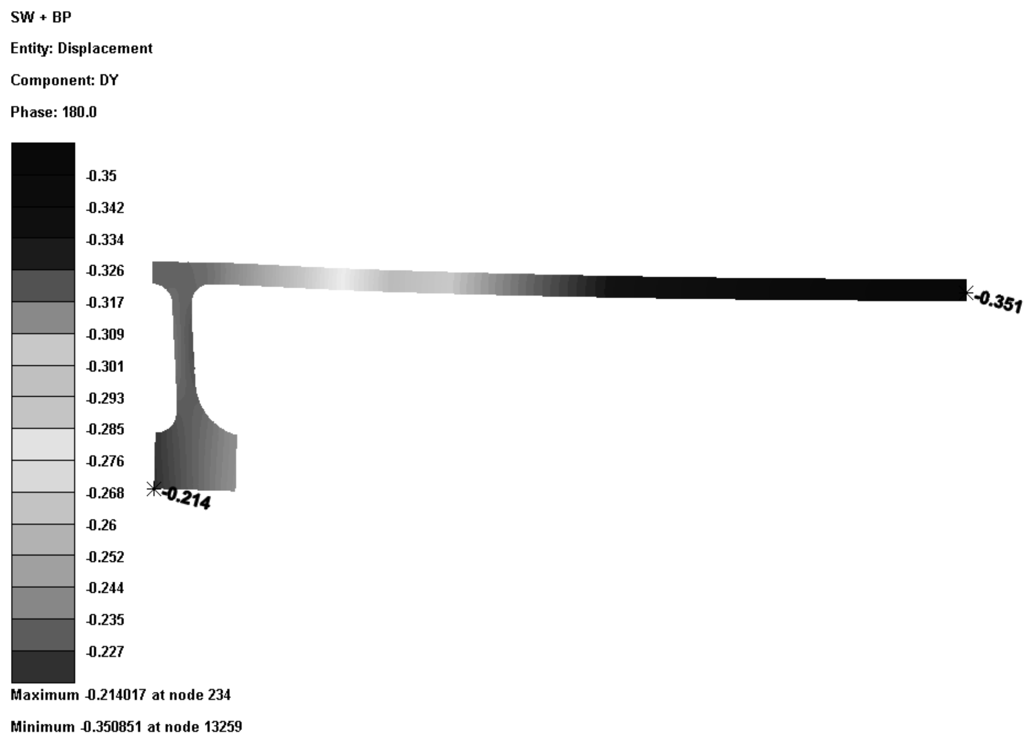

Figure 20. Contour plot of the maximum radial displacement of the pulley shell

The contour plot of the von Mises stress in the pulley shell is shown in Figure 21:

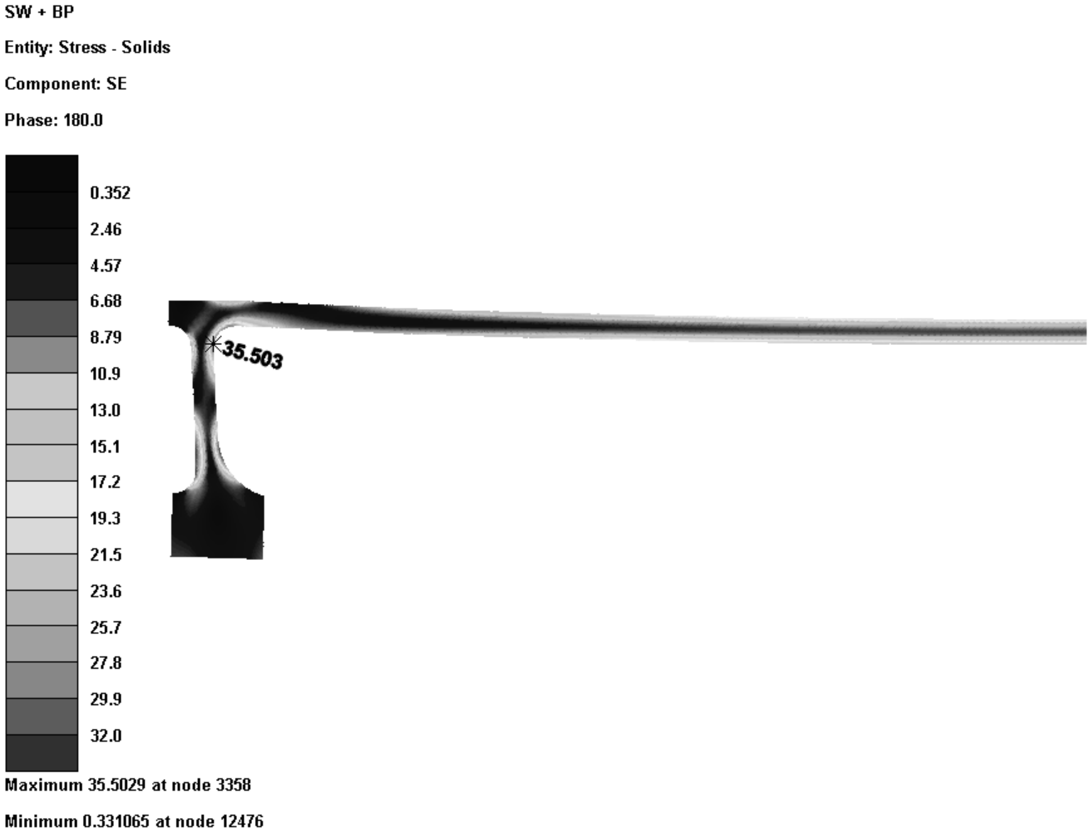

Figure 21. Contour plot of the von Mises stress in the pulley shell

6. COMPARISON OF A CURRENT DESIGN METHOD TO THE NUMERICAL STUDY

The current design techniques assess the components of the pulley separately and not as a homogenous structure. The comparison of the current design techniques and FEA conducted in the study is compared and conclusions drawn.

The current design technique by King [4] revealed the following results for the pre-selected pulley versus the Finite Element Analysis study conducted.

The static stress results are as follows:

Type of Stress	Current Design Method	FEA
Hoop stress in the shell due to the locking element	32.4 MPa	33.4 MPa

The fatigue results are as follows:

Position of Stress Range	Current Design Method	FEA
Shell Longitudinal Seam Weld	13.2 MPa	34.82 MPa
Shell to End Disk Circumferential Weld	23.9 MPa	38.50 MPa

The static results for the comparison indicate excellent correlation between the current design criteria and the numerical work conducted for the shell. The fatigue assessment however, revealed a large difference in the results with the current design criteria being less conservative than the numerical work, most likely due to the small angle of wrap used in the study as well as the distribution of the stress and stiffness of the T-Bottom type end disk.

The difference in the stress ranges determined is due to the inability of the theory implemented in the design criteria to accurately calculate the stresses in the shell-to-end disk interface [[6] due to the separate assessment of the components in the design criteria as compared to the FEA.

7. FATIGUE PERFORMANCE OF THE PULLEY

The fatigue performance of the pulley is assessed upon completion of a steady-state static analysis of the conveyor pulley assembly. A pulley typically rotates 35 million times per year [19]. The selected pulley in this study would need to sustain over 50 million cycles per year for 24 hours per day and 365 days of operation and hence the components should be designed for infinite fatigue life.

This study was conducted to investigate the influence of the operational loads, assembly loads and the residual stresses due to the manufacturing process on the fatigue performance of the pulley. This required the following steps:

- Determination of the stress ranges at the measurement positions and machined positions for the operational load case. The assembly and manufacturing load cases contributed to the mean stress effect for the fatigue assessment
- Determination of the endurance limits of the welds according to the international fatigue weld standards currently used in industry. The fatigue resistance curves were based on the types used by Lill [15]. The equivalent fatigue resistance curves were then chosen from the other fatigue codes
- Determination of the modified endurance limits of the machined areas according to fundamental fatigue theory
- Check for the possibility of residual stress relaxation upon fatigue loading.

This example of the bending stress range in the shell indicates a cycle with constant amplitude as shown in Figure 22:

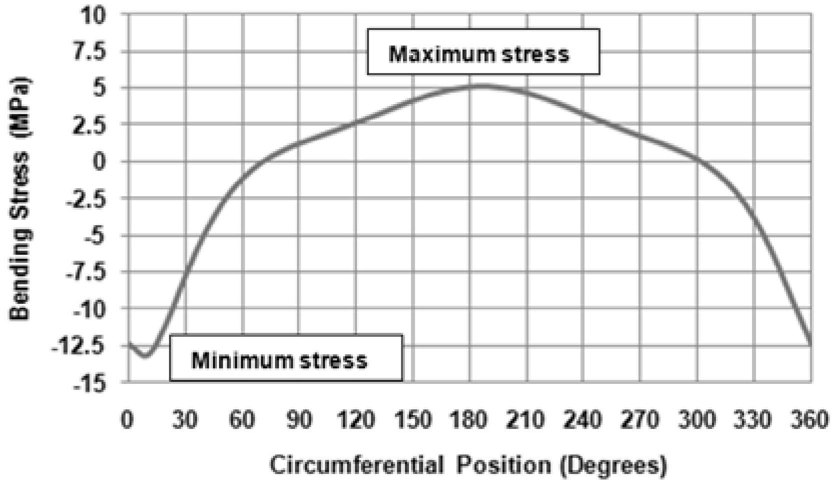

Figure 22. Constant amplitude bending stress range

The stress range is then determined from the difference of the maximum and minimum stresses as follows:

$$\Delta\sigma_R = \sigma_{MAX} - \sigma_{MIN}$$

Weld measurement positions for the as-welded condition of the pulley are shown in Figure 23:

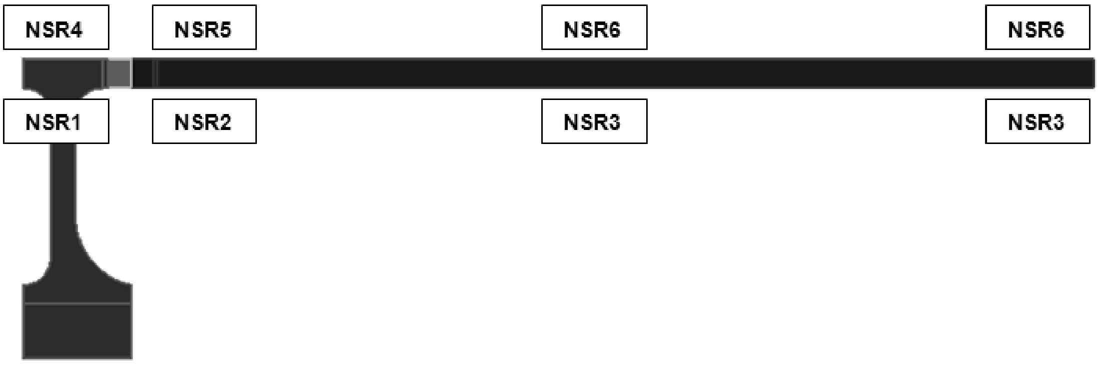

Figure 23. Weld measurement position of the pulley

Weld measurement positions for the stress relieved condition of the pulley as shown in Figure 24:

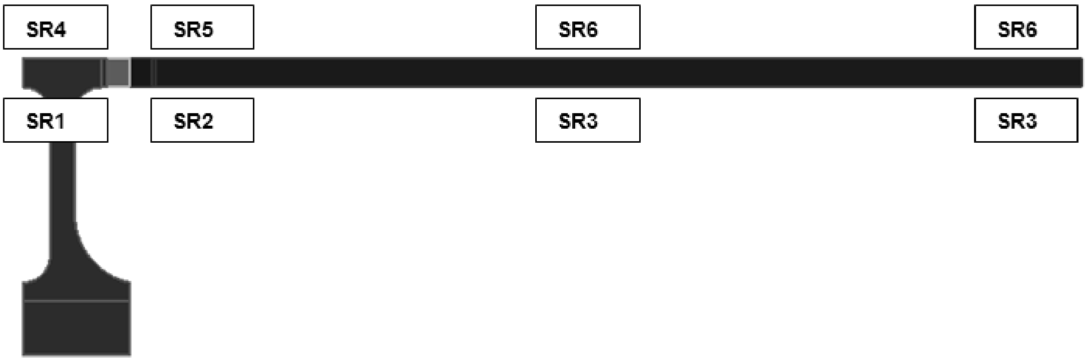

Figure 24. Weld measurement position of the pulley

Machined measurement positions for the stress relieved condition of the pulley are shown in Figure 25:

Figure 25. Machined measurement position of the pulley

The surface finishes of the components for the pulley assembly are shown in Table 12:

Component	ISO Designation	Surface Roughness (μm)
Locking Element	N7	1.6
End Disk	N8	3.2
Shaft	N8	3.2
Shell	N10	12.5

Table 12. Surface finishes of the components for the pulley assembly [24]

7.1 Residual Stress in Welds

Residual stresses introduced due to welding can be close to the yield strength of the material and as such can be detrimental to the fatigue resistance of a joint [9]. Tensile residual stresses thus induced will cause an effective tensile mean stress and hence decrease the fatigue life at the joint at the weld toe of interest. Therefore the fatigue life of as-welded joints has limited sensitivity to the applied mean stress caused by the operational loading due to the fact that when these stresses are added to the residual stresses, the maximum stress will have a value close to the yield strength of the material regardless of the mean stress level associated with the applied loads [9].

The effect of residual stress on the stress cycle of an as-welded joint is shown in Figure 26:

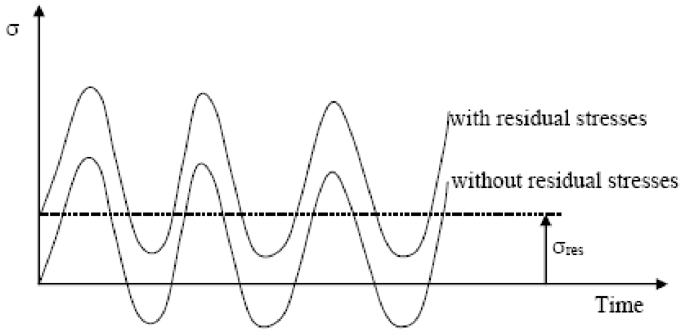

Figure 26. Influence of the residual stress on a stress cycle of an as-welded joint [9]

Dependency on the applied mean stress due to the operational load has been found for stress relieved joints as is shown in Figure 27:

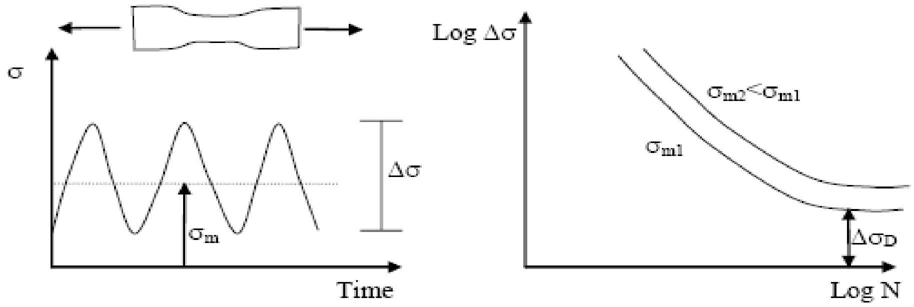

Figure 27. Tensile mean stress due to the loading as in a stress relieved joint [9]

Stress relieved joints are less vulnerable if the stress cycle due to the applied loading is partly compressive [9]. The next section will show the allowance of this benefit in the fatigue standards considered.

7.2 Fatigue Assessment According to Standards

The international weld fatigue standards currently used by industry were considered for the assessment of the fatigue resistance of the joints of interest.

The classifications of the circumferential and longitudinal seam weld were taken from BS 7608 [21] as suggested by Lill [15].

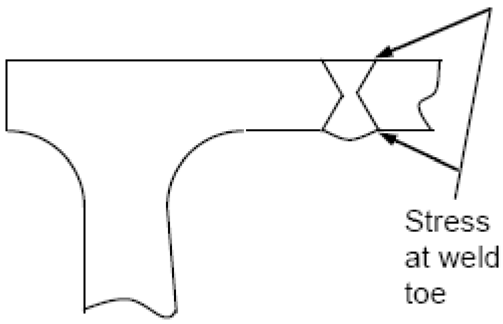

Figure 28. Perpendicular stress measured at the weld toe of the butt weld [15]

The classification of the butt weld details with stress range extracted perpendicular to the weld toe for T-Bottom type pulley according to BS 7608 as indicated in Table 13:

Weld Location	Weld Class	Type Number	Endurance Limit (MPa)
Longitudinal butt weld	D	6.2	53
Circumferential weld	D	6.2	53

Table 13. Weld classification according to BS 7608 [21]
Note 2: **Class D applicable if both sides of the butt weld are machined or ground flush**

The main criteria being that the stress cycle at the weld toe should be below the constant amplitude endurance limit (stress range) of the joint under consideration. This would then comply with the condition that the joint theoretically could sustain an infinite number of cycles and hence fatigue need not be considered.

A stress cycle below the constant amplitude endurance limit of a joint is shown in Figure 29:

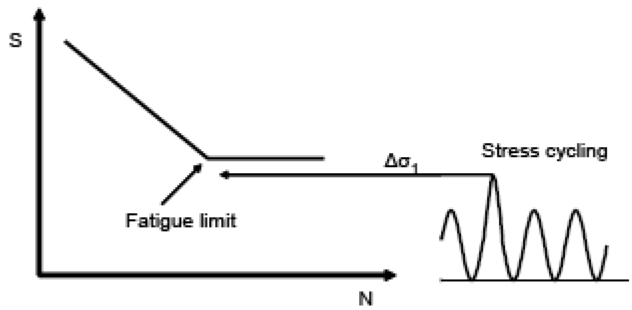

Figure 29. Stress cycle below the endurance limit of a joint [20]

The codes consider the mean stress effect of stress relieved joints in a similar manner which are shown as follows:

BS 7608 [21] and BS EN1993-1-9 [22] indicate the reduction of the compressive portion of the stress range for a stress relieved joint as shown in Figure 30:

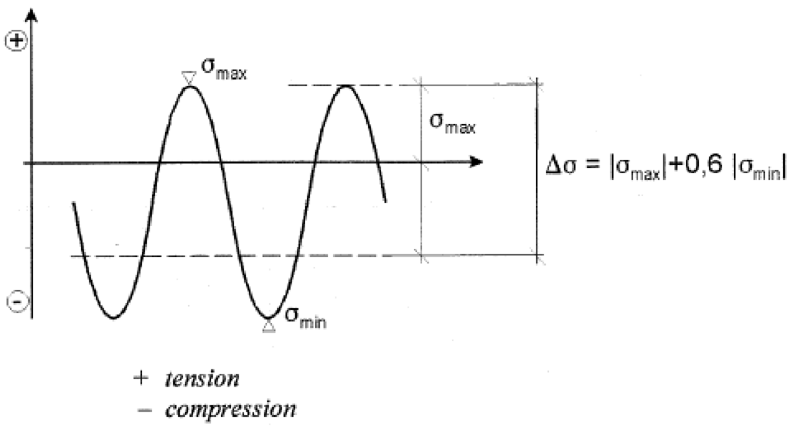

Figure 30. Reduction of the stress range due to stress relieving [22]

DNV-RP-C203 [20] allows a reduction factor for the compressive portion of the stress cycle for a stress relieved joint as shown in Figure 31:

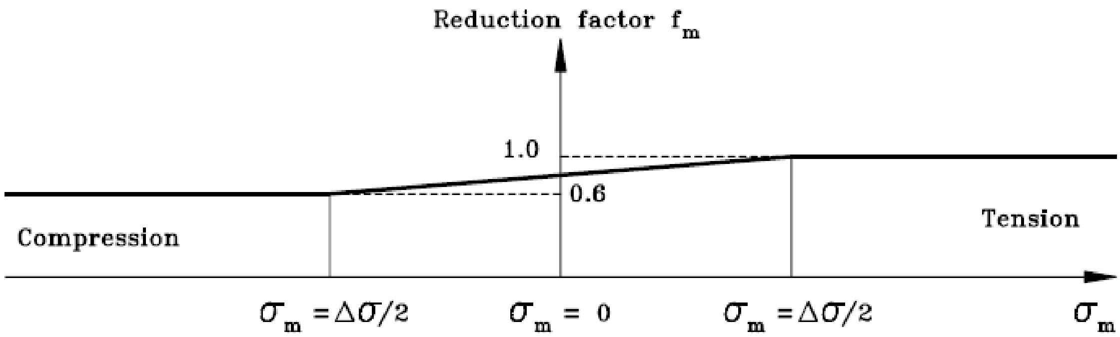

Figure 31. Reduction factor of the stress cycle for stress relieving [20]

$$f_m = \frac{\sigma_{MAX} + 0.6\sigma_{MIN}}{\sigma_{MAX} + \sigma_{MIN}}$$

IIW-1823-07 [23] states that for stress ratios less than 0.5, a fatigue enhancement factor may be multiplied with the fatigue resistance curve of interest. The fatigue enhancement factor depends on the level and direction of the residual stress in the joint.

For stress relieved joints with residual stress lower than 20% of the yield strength of the material, the following fatigue enhancement factors may be used based on the stress ratios under consideration:

$$R = \frac{\sigma_{MIN}}{\sigma_{MAX}}$$
$$f(R) = 1.6 \, for \, R < -1$$
$$f(R) = -0.4R + 1.2 \, for - 1 \leq R \leq 0.5$$
$$f(R) = 1 \, for \, R > 0.5$$

7.3 Results of the Fatigue Assessment

The result of the fatigue assessment according to the standards is as follows. The set of results revealing the greatest fatigue ratio were herein reported:

$$FR = \frac{\Delta\sigma_R}{\sigma_{EL}}$$

The fatigue ratio in the hoop direction for the as-welded condition for BS EN1993-1-9 is shown in Table 14:

Position	NSR6	NSR3	NSR6	NSR3
Stress Range (MPa)	30.340	30.610	34.820	35.600
Endurance Limit (71) (MPa)	52.327	52.327	52.327	52.327
Fatigue Ratio	58%	59%	67%	68%

Table 14. Fatigue ratio in the hoop direction for the as-welded condition

Position	NSR4	NSR5	NSR1	NSR2
Stress Range (MPa)	30.100	7.320	38.500	14.700
Endurance Limit (71) (MPa)	52.327	52.327	52.327	52.327
Fatigue Ratio	58%	14%	74%	28%

Table 15. Fatigue ratio for BS EN1993-1-9 in the axial direction for the as-welded condition

Position	SR6	SR3	SR6	SR3
Stress Range (MPa)	21.140	26.966	24.500	31.240
Endurance Limit (71) (MPa)	52.327	52.327	52.327	52.327
Fatigue Ratio	40%	52%	47%	60%

Table 16. Fatigue ratio for BS EN1993-1-9 in the hoop direction for the stress relieved condition

Position	SR4	SR5	SR1	SR2
Stress Range (MPa)	25.300	5.644	29.180	11.484
Endurance Limit (71) (MPa)	52.327	52.327	52.327	52.327
Fatigue Ratio	48%	11%	56%	22%

Table 17. Fatigue ratio for BS EN1993-1-9 in the axial direction for the stress relieved condition

The fatigue assessment according to BS EN 1993-1-9 revealed the most conservative results based on the lower endurance limit for the fatigue resistance detail considered. The greatest fatigue ratio was 74% for the as-welded joint NSR1 in the axial direction.

The corrected endurance limit for the machined areas of concern is as follows:

$$FR = \frac{\Delta\sigma_A}{\sigma_{EL}}$$

Position	MS1	MS2	MS3	MS4
Stress amplitude (MPa)	19.300	26.300	39.600	35.000
Endurance limit under zero mean stress (MPa)	110.782	110.782	110.782	110.782
Mean Stress (MPa)	9.576	-50.183	-86.927	-72.012
Ultimate Tensile Strength (MPa)	479.530	479.530	479.530	479.530
Endurance limit under mean stress (MPa)	108.569	110.782	110.782	110.782
Fatigue Ratio	18%	24%	36%	32%

Table 18. Fatigue ratio in the radial direction

Position	MS1	MS2	MS3	MS4
Stress amplitude (MPa)	5.545	4.495	13.750	15.700
Endurance limit under zero mean stress (MPa)	110.782	110.782	110.782	110.782
Mean Stress (MPa)	57.836	33.390	108.478	129.487
Ultimate Tensile Strength (MPa)	479.530	479.530	479.530	479.530
Endurance limit under mean stress (MPa)	97.420	103.068	85.721	80.867
Fatigue Ratio	6%	4%	16%	19%

Table 19. Fatigue ratio in the hoop direction

7.4 Residual Stress Relaxation Due to Fatigue

The presence of plastic deformation of the weld toe during fatigue cycling is thought to cause the relaxation behaviour of residual stress [25].

Mochizuki et al. [25] found that for a high stress range the magnitude of the residual stresses was relaxed during the initial fatigue cycles. For the low stress ranges, fatigue strength depends on the initial residual stress because the residual stress changes only slightly due to the fatigue loading.

Based on these findings, consideration of residual stress relaxation can be made if the following condition is met (ignoring strain hardening):

$$\sigma_{RES} + \sigma_{MAX} > \sigma_Y$$

The initial measured residual stresses for this study were found not to undergo relaxation as the sum of the initial residual stress and maximum stress was below the yield strength of the material.

8. CONCLUSION

The residual stress measurements conducted indicated a large reduction of residual stress levels due to the stress relieving. The non-uniform stress method according to ASTM E837-08 was found to be the most accurate for the stress distribution vs. depth considered. Fourier analysis of the pulley was shown to be an accurate means of determining the displacements and stresses in the structure. The comparison of the FEA of the selected pulley with King's design criteria indicates good correlation in the static results. The fatigue results indicate discrepancies compared to the numerical work. The fatigue assessment was considered based on international standards used by industry. All of the details considered were found to have stress ranges below their respective endurance limits and hence infinite fatigue life is expected. BS EN 1993-1-9 was found to be the most conservative for the study. The IIW-1823-07 is however, the more thorough and up-to-date of the fatigue standards used in the investigation. Residual stress relaxation was found to not have occurred due to the fact that the sum of the initial residual stress and the maximum stress was below the yield strength of the material for the details and specification of pulleys considered.

9. RECOMMENDATIONS

An experimental and numerical program should be set up to determine where the maximum residual stress is placed around the circumference of the pulley. An evaluation of the residual stress state due to machining in the areas of concern should be conducted. The ease of model construction and run time indicated that Fourier analysis of this type of structure is suitable for implementation in the design procedure of pulleys. It is therefore recommended that FE systems be used during the design and selection of pulleys due to their affordability as compared to 20 years ago.

The comparison of the numerical results with King's model reveals discrepancies with regards to the stress components determined for the fatigue assessment. It must however, be remembered that the model was developed for pulley checks at design office level and hence was not meant as a detailed design tool. The modern IIW-1823-07 permits the factoring of the fatigue resistance curve based on the residual stress state in the weld detail of concern. Based on these recently implemented findings in this standard, it would be possible to take advantage of the effect of the reduction in residual stress levels due to stress relieving and hence allow thinner shell thicknesses as well as further optimised end disks to be implemented in the design of pulleys. This could result in lighter and more affordable pulleys being made available to the end user. A test program should be conducted to investigate experimentally and numerically the possible design gains in this regard. The evaluation of residual stress relaxation should be included in the pulley design criteria. This study should be extended to investigate the residual stress levels and fatigue in the turbine-type pulley configuration.

ACKNOWLEDGEMENTS

The authors wish to acknowledge the support of the University of Johannesburg, Mechanical Engineering Science Department with regards to financial support and facilities for the project. Professor R F Laubscher for his valued guidance and assistance in this work. CPM Engineering who supplied the shell for the experimental work as well as the pulley information that was used for the study. William Rall and Professor Danie Hattingh of the Nelson Mandela Metropolitan University for the supply and assistance with the incremental hole-drill testing.

NOMENCLATURE

MRD	Maximum radial displacement (mm)
TV	Target value (mm)
PD	Percentage difference (%)
T T1 T2	Belt tension (kN)
D	Outer diameter of the pulley (mm)
W	Belt width (mm)
IHP	Interface hub (end disk) pressure (MPa)
TV	Target value (MPa)
$\Delta\sigma_A$	Stress amplitude (MPa)
$\Delta\sigma_R$	Stress range (MPa)
σ_{MAX}	Maximum stress (MPa)
σ_{MIN}	Maximum stress (MPa)
f_m	Mean stress reduction factor
f(R)	Fatigue enhancement factor
FR	Fatigue ratio
σ_{EL}	Endurance limit for constant amplitude stress range and stress amplitude (MPa)
σ_{RES}	Initial residual stress (MPa)
σ_Y	Yield strength (MPa)
R	Stress ratio

REFERENCES

[1] www.ckit.co.za/secure/conveyor/troughed/pulleys/pulleys_beginners_2basics.htm

[2] Lange H, “Investigation in Stressing of Conveyor Belt Drums”. Thesis for a Doctorate in Engineering, Hannover, 1963

[3] Schmoltzi W, “Designing Drums with Transverse Shafts for Belt Conveyors”. Thesis for Doctorate in Engineering, Hannover, 1974

[4] King T J, “The Function and Mechanism of Conveyor Pulley Drums”. Beltcon 3, 1985

[5] Qiu X, Sethi V, “A New Pulley Stress Analysis Method Based on Modified Transfer Matrix”, Bulk Solids Handling Trans Tech Publications, Vol. 13, No. 4, 1993,

[6] Sethi V, Nordell L K, “Modern Pulley Design Techniques and Failure Analysis Methods”, AIME-SME Annual Convention, Reno, Nevada, 1993

[7] www.ckit.co.za/secure/conveyor/troughed/pulleys/pulleys_beginners_2basics.htm

[8] Stephens R I, Fatemi A, Stephens R R, Fuchs H O, “Metal Fatigue in Engineering”, John Wiley and Sons Inc., Second Edition, 2001

[9] Lassen T, Recho N, “Fatigue Life Analyses of Welded Structures”, ISTE, 2006

[10] Mathar, J., Determination of Initial Stresses by Measuring the Deformation around Drilled Holes, *Trans., ASME* **56** (4), pp. 249 - 254, 1934

[11] E837-08, “Standard Test Method for Determining Residual Stresses by the Hole-Drilling Strain-Gage Method”, ASTM International, 2008

[12] Paulo de Tarso V. Gomes, Nelson N.A. Filho, Denis Henrique B. Scaldaferri, Geraldo A.S. Martins, Alexandre Q. Bracarense, Tanius R. Mansur, Residual Stress Measurements by the Blind-hole Drilling Method in a Dissimilar Welded Sheet Metal-Carbon Steel ASTM A 36 and AISI 304 Stainless Steel, with AISI 316 L Filler Metal, Centro de Desenvolvimento da Tecnologia Nuclear, 2010

[13] Grant P V, Lord J D, MATC(MN)31, “An Evaluation of Four Hole Drilling Analysis Techniques with respect to Non-Uniform Residual Stress Fields”, 2002

[14] CPM Engineering “Pulley T-Bottom and Locking Element” Brochure

[15] Lill A, “Conveyor Pulley Design”. Beltcon 14, 2007

[16] LUSAS@ “Modeller Reference Manual”, LUSAS Version 14.5 : Issue 1, 2011

[17] LUSAS@ “Theory Manual Volume 1 and 2”, LUSAS Version 14.4 : Issue 1, 2010

[18] Ravikumar M, Chattopadhyay A, “Integral analysis of conveyor pulley using finite element method”, Computers and Structures 71, pp. 303 – 332, 1999

[19] Perry R T, “Some Aspects of Conveyor Pulley Design”, Jegkurt Engineering, 1986

[20] DNV-RP-C203, “Fatigue Design of Offshore Steel Structures”, DET NORSKE VERITAS (DNV), 2005

[21] BS 7608 : 1993, “Code of Practice for Fatigue Design and Assessment of Steel Structures”, BSI, 1999

[22] BS EN1993-1-9:2005, “Eurocode 3 : Design of Steel Structures – Part 1-9 : Fatigue”, BSI, 2006

[23] Hobbacher A, IIW document IIW-1823-07 “Recommendations for Fatigue Design of Welded Joints and Components”, International Institute of Welding (IIW), 2008

[24] ISO 1302 : 2002, “Indication of surface texture in technical product documentation”, 2002

[25] Mochizuki M, Hattori T, Nakakado K, “Residual stress reduction and fatigue strength improvement by controlling welding pass sequences”, ASME pp. 108-112, 2000

BIBLIOGRAPHY

1. Grant P V, Lord J D, Whitehead P S, “No.53 Measurement Good Practise Guide, “Measurement of Residual Stress by the Incremental Hole-Drilling Technique”, National Physical Laboratory, 2002
2. Schajer G S, “Hole-Drilling Residual Stress Profiling with Automated Smoothing”, Journal of Engineering Materials and Technology, Vol. 129, No. 3, pp. 440 – 445, 2000
3. Schajer G S, “Measurement of Non-Uniform Residual Stresses Using the Hole Drilling Method”, Journal of Engineering Materials and Technology, Vol. 110, No. 4, Part 1 : pp. 440 – 445, Part 2 : pp. 344 - 349, 1988
4. Tech Note TN-503, “Measurement of Residual Stress by the Hole-Drilling Strain Gauge Method”, Vishay Micro-Measurements, 15 Aug 2007

ABOUT THE AUTHORS

GARY STYGER

Gary Styger holds a Bachelor’s in Mechanical Engineering Technology from Wits Technikon. He is currently busy with a Master’s in Philosophy in Mechanical Engineering Science at the University of Johannesburg. He works for Weir Minerals Africa in the vibratory screens division as a Mechanical Design Engineer

Gary Styger

Weir Minerals Africa
31 Isando Rd.
Isando
Email: gary.styger@gmail.com

PROFESSOR RUDOLPH LAUBSCHER

Rudolph Laubscher holds a Bachelor’s, Master’s and Doctorate in Mechanical Engineering Science from the Rand Afrikaans University. He is currently an Associate Professor in the School of Mechanical Engineering at the University of Johannesburg where his main research interests are in the fields of physical metallurgy, strength of materials, finite element analysis and manufacturing. He has over 20 years of combined industry and academic experience and consults widely in the industry as a failure and structural analyst.

Professor R F Laubscher

University of Johannesburg
Faculty of Engineering and the Built Environment
Mechanical Engineering Science
Auckland Park Kingsway Campus
Johannesburg
Email: rflaubscher@uj.ac.za